

Clot Contraction Drives the Translocation of Procoagulant Platelets to Thrombus Surface

Dmitry Y. Nechipurenko,* Nicolas Receveur,* Alena O. Yakimenko, Taisiya O. Shepelyuk, Alexandra A. Yakusheva, Roman R. Kerimov, Sergei I. Obydennyy, Anita Eckly, Catherine Léon, Christian Gachet, Ekaterina L. Grishchuk, Fazoil I. Ataullakhanov, Pierre H. Mangin,† Mikhail A. Panteleev†

Objective—After activation at the site of vascular injury, platelets differentiate into 2 subpopulations, exhibiting either proaggregatory or procoagulant phenotype. Although the functional role of proaggregatory platelets is well established, the physiological significance of procoagulant platelets, the dynamics of their formation, and spatial distribution in thrombus remain elusive.

Approach and Results—Using transmission electron microscopy and fluorescence microscopy of arterial thrombi formed in vivo after ferric chloride–induced injury of carotid artery or mechanical injury of abdominal aorta in mice, we demonstrate that procoagulant platelets are located at the periphery of the formed thrombi. Real-time cell tracking during thrombus formation ex vivo revealed that procoagulant platelets originate from different locations within the thrombus and subsequently translocate towards its periphery. Such redistribution of procoagulant platelets was followed by generation of fibrin at thrombus surface. Using in silico model, we show that the outward translocation of procoagulant platelets can be driven by the contraction of the forming thrombi, which mechanically expels these nonaggregating cells to thrombus periphery. In line with the suggested mechanism, procoagulant platelets failed to translocate and remained inside the thrombi formed ex vivo in blood derived from nonmuscle myosin (*MYH9*)-deficient mice. Ring-like distribution of procoagulant platelets and fibrin around the thrombus observed with blood of humans and wild-type mice was not present in thrombi of *MYH9*-knockout mice, confirming a major role of thrombus contraction in this phenomenon.

Conclusions—Contraction of arterial thrombus is responsible for the mechanical extrusion of procoagulant platelets to its periphery, leading to heterogeneous structure of thrombus exterior.

Visual Overview—An online [visual overview](#) is available for this article. (*Arterioscler Thromb Vasc Biol.* 2019;39:37-47. DOI: 10.1161/ATVBAHA.118.311390.)

Key Words: aorta ■ ferric chloride ■ fibrin ■ mice ■ thrombosis

Accumulation and activation of platelets at the site of vascular injury is required for primary hemostasis, but may also result in thrombosis. Activation of platelets is a multistep process, which depends on local biochemical and mechanical environments.¹ In general, activated platelets form at least 2 subpopulations with distinct traits and, possibly, different functions.²⁻⁷ The first subpopulation is characterized by complex morphological changes, activation of integrins that mediate aggregation, and low, if any, phosphatidylserine externalization. These well-aggregating platelets are likely responsible for the actual build up of thrombus and clot contraction.^{7,8} The second subpopulation is observed only on potent activation and is usually called procoagulant platelets because their

membrane can accelerate membrane-dependent coagulation reactions (it was alternatively called coated platelets, necrotic platelets, sustained calcium-induced platelets, etc^{3,5-7,9-11}). Although there are indications that not all procoagulant platelets are similar,¹²⁻¹⁵ they all are generally believed to possess spherical shape, disrupted cytoskeleton, low integrin activity, and high level of phosphatidylserine externalization,^{2,3,6,7,9,12,12a,16} which promotes binding of coagulation factors and leads to dramatic acceleration of coagulation reactions.^{6,10,11,17,18}

See accompanying editorial on page 5

The (patho)physiological role of procoagulant platelets remains a subject of active debate, with some studies favoring

Received on: June 9, 2018; final version accepted on: October 16, 2018.

From the Department of Physics (D.Y.N., R.R.K., F.I.A., M.A.P.) and Faculty of Basic Medicine (T.O.S.), Lomonosov Moscow State University, Russia; Dmitry Rogachev National Research Center of Pediatric Hematology, Oncology, and Immunology, Moscow, Russia (D.Y.N., A.O.Y., T.O.S., A.A.Y., S.I.O., F.I.A., M.A.P.); Center for Theoretical Problems of Physicochemical Pharmacology, Moscow, Russia (D.Y.N., A.O.Y., T.O.S., A.A.Y., S.I.O., F.I.A., M.A.P.); INSERM, Etablissement Français du Sang-Grand Est, UMR_S1255, Fédération de Médecine Translationnelle de Strasbourg, Université de Strasbourg, France (N.R., A.E., C.L., C.G., P.H.M.); Department of Physiology, Perelman School of Medicine, University of Pennsylvania, Philadelphia (E.L.G.); and Department of Biological and Medical Physics, Moscow Institute of Physics and Technology, Dolgoprudny, Russia (F.I.A., M.A.P.).

*D.Y. Nechipurenko and N. Receveur contributed equally as first authors.

†P.H. Mangin and M.A. Panteleev contributed equally as senior authors.

The online-only Data Supplement is available with this article at <https://www.ahajournals.org/doi/suppl/10.1161/ATVBAHA.118.311390>.

Correspondence to Mikhail A. Panteleev, DSc, Department of Physics, Lomonosov Moscow State University, 1 Samory Mashela St, Moscow, Russian Federation. Email mapanteleev@yandex.ru

© 2018 American Heart Association, Inc.

Arterioscler Thromb Vasc Biol is available at <https://www.ahajournals.org/journal/atvb>

DOI: 10.1161/ATVBAHA.118.311390

Nonstandard Abbreviations and Acronyms

DIC	differential interference contrast
WT	wild-type

prohemostatic^{19–23} or prothrombotic roles,^{24–26} and others suggesting an antithrombotic function because of the antiaggregatory phenotype of these cells.^{27,28} The data on the location of procoagulant platelets in arterial thrombi are also controversial. Munnix et al¹⁹ reported separate patches of procoagulant platelets distributed throughout the thrombi formed *in vitro* and *in vivo*. However, Hua et al²⁶ did not find procoagulant platelets after laser-induced injury of cremaster muscle arterioles in mice, although they were present and partially colocalized with fibrin in FeCl₃-induced occlusive injury of the same vessels with irregular spatial distribution. A study using laser injury of mesenteric venules described procoagulant platelets and fibrin to be colocalized in the central region of the thrombus.²⁹ However, recent data on the mechanism of pulmonary thrombosis after gut ischemia uncovered the importance of neutrophil interactions with procoagulant platelets on the surface of thrombi.³⁰ Moreover, early reports on morphology of the hemostatic plugs formed in dogs and humans detected some ballooned platelets (which is a key feature of the procoagulant platelets morphology) and fibrin on the surface of these plugs.^{31,32} Such surface localization of procoagulant platelets might seem paradoxical because local biochemical environment near thrombus surface should not favor the formation of procoagulant platelets, which requires potent activation. Such potent activation would be reasonable to expect in the inner parts of the thrombus, rather than the periphery. To elucidate physiological distribution of procoagulant platelets, we investigated their localization in thrombi formed after different injury types *in vivo* and revealed their robust surface localization. To get further insights into the mechanism leading to this nonintuitive localization, we used our previously developed *ex vivo* system, in which the dynamics of single procoagulant platelets can be observed in thrombi formed during blood perfusion over a collagen-bearing surface.

Materials and Methods

The data that support the findings of this study are available from the corresponding author on reasonable request.

In Vivo Models of Arterial Thrombosis

The abdominal aorta of anesthetized mice aged 8 to 10 weeks was exposed and mechanically injured by pinching with forceps (type 11063-07; Fine Science Tools, Heidelberg, Germany), as described in Schaff et al.³³ The FeCl₃-injury was performed, as in Eckly et al.³⁴ Briefly, the common carotid artery of 8- to 10-week old anesthetized mice were exposed, and the left carotid artery was injured by applying a patch of filter paper (1M Whatmann) saturated with 7.5% FeCl₃ for 2 minutes. Injured vessels were processed and imaged using electron transmission microscopy as described in Eckly et al.³⁴ or fluorescence microscopy. The details of vessel processing, transmission electron microscopy, and fluorescent imaging are given in Methods in the [online-only Data Supplement](#). Both female and male mice were chosen for these experiments. The studied phenomenon was observed for both sex types, and data were combined independent on sex. Approximately equal fraction of female and male mice was studied for all mice models described here.

Real-Time Platelet Dynamics Ex Vivo Observed With Confocal Microscopy

The protocols for preparation of glass microslides covered with collagen, flow chambers, and human blood for perfusion are described in Methods in the [online-only Data Supplement](#). Blood supplemented with fluorescent probes was perfused at flow rates corresponding to shear rates 200 and 1000 s⁻¹, as described in Abaeva et al.¹² Confocal images of platelet aggregates were acquired with an Axio Observer Z1 microscope (Carl Zeiss, Jena, Germany) equipped with a ×100 microscopic objective. A 639-nm laser was used for excitation of Alexa647-labeled annexin V and a 488-nm laser for fluorescein isothiocyanate–coupled antibodies. Images were analyzed with ImageJ software and 3-dimensional Viewer plugin (National Institute of Health, Bethesda).

Fibrin Formation on Collagen Under Flow Conditions

To observe real-time fibrin formation, mouse blood was collected on citrate before being recalcified. Citrated mouse blood in the presence of annexin V–fluorescein isothiocyanate (10 µg/mL) was recalcified with 12 mmol/L calcium chloride (3.7 mmol/L of magnesium chloride was also added to restore physiological concentration of free magnesium ions) before being perfused over collagen. Fluorescent images were captured in epifluorescence mode using the Leica DMI 4000 B microscope (Leica Microsystems) and Metamorph software (Molecular Devices, Sunnyvale, CA). To detect fibrin formation, blood was supplemented with the DyLight650-coupled antifibrin antibody 59d8 (5 µg/mL) that was kindly provided by Dr Christophe Dubois (Inserm UMR_S11076, Marseille). In experiments for confocal imaging of thrombus structure, platelets were also labeled with DiOC6 (3,3'-dihexyloxycarbocyanine iodide; 1 µmol/L).

Computational Modeling of Platelet Motion During Contraction

Platelets were treated as elastic spheres, and their interaction was modeled with Morse potential.^{34a} Thrombus contraction process was modeled as slow decrease in equilibrium distance of Morse potential which resulted in increase of platelet packing density because of decrease of mean interplatelet distance within the aggregate. Detailed description of computational model and its parameters is given in the [online-only Data Supplement](#).

Statistical Analysis

All statistical analyses were performed using GraphPad Prism program, version 6.0 (Prism, GraphPad, La Jolla, CA). All values are reported as mean±SEM in case of normal distribution or median in case of nonnormal distribution. Data between 2 groups were compared by the Mann-Whitney *U* test; *P* value (<0.01) was chosen as the cutoff level for statistical significance (2-tailed), unless another value is indicated.

Results

Procoagulant Platelets Are Found at the Surface of Thrombi Formed In Vivo in the Large-Artery Experimental Models of Thrombosis

To study spatial distribution of procoagulant platelets in thrombi formed *in vivo*, we induced arterial thrombosis in mice by creating FeCl₃-injury of the carotid artery. The mice were euthanized, the injured vessels were fixed, and analyzed with transmission electron microscopy or fluorescence microscopy, revealing a heterogeneous thrombus composition. The highly contracted and tightly packed platelets were found close to the site of FeCl₃ application, whereas the less activated platelets, as judged by the presence of granules,

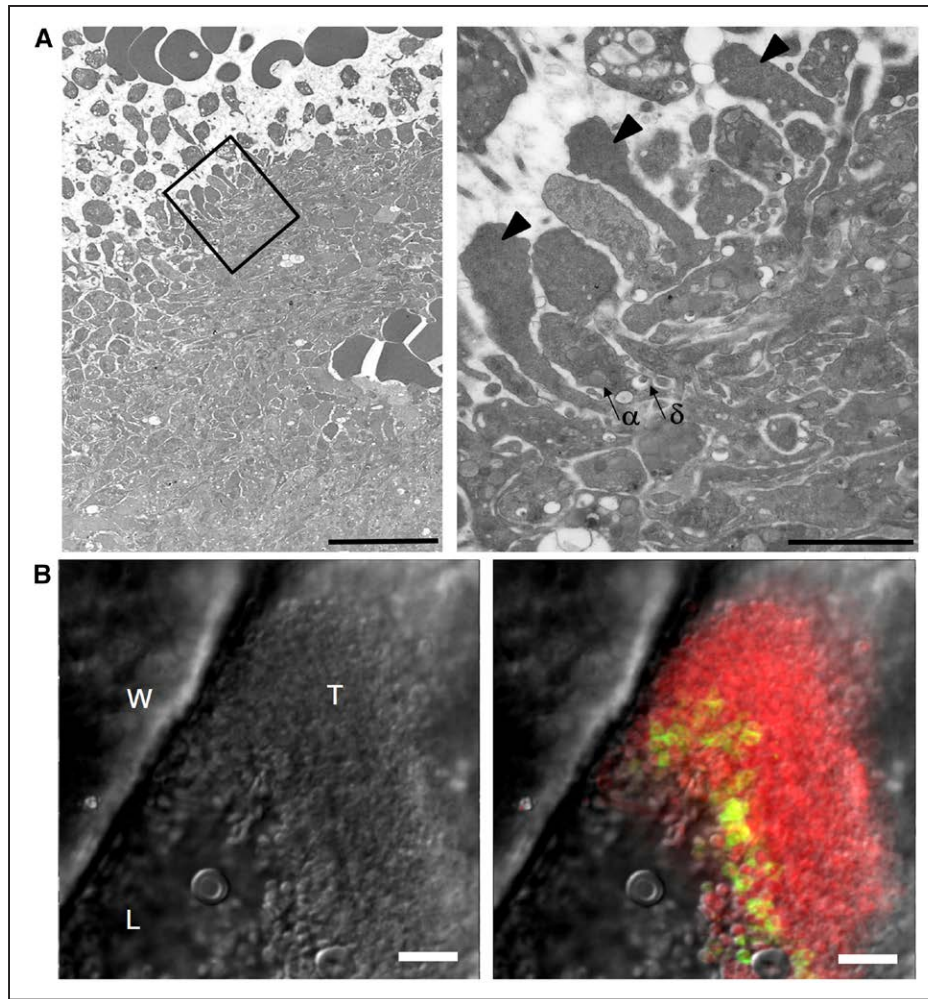


Figure 1. Localization of procoagulant platelets in thrombi formed in vivo. **A**, Bigger- and smaller-scaled transmission electron microscopy images of ferric chloride-induced thrombi in carotid artery of the wild-type (WT) mice. Black triangles mark the positions of the procoagulant platelets distinguished by their unique morphology, whereas arrows show alpha and dense granules. Left and right scale bars are 10 and 2 micrometers, respectively. **B**, Optical images of thrombi formed after ferric chloride-induced injury of carotid artery of WT mice. **Left** image corresponds to the differential interference contrast (DIC) channel, whereas the **right** image represents superposition of the DIC and confocal fluorescent images corresponding to annexin V–Alexa647 (green) and DiOC6 (3,3'-dihexyloxycarbocyanine iodide; red). The vessel wall, lumen, and thrombus are designated as W, L, and T, respectively. Scale bars are 10 μm .

were localized near the lumen, suggesting a gradient of activation spreading from the core of thrombus to its surface (Figure 1A, left). The procoagulant platelets were readily identified within the stable thrombus, thanks to their unique morphology^{18,35}: the elongated shape and sparse intracellular densities (Figure 1A, right). Interestingly, this type of platelets was specifically located at thrombus periphery, consistent with recent findings³⁰ and earlier reports.^{31,32} Preferential surface distribution of procoagulant platelets in this injury model was confirmed by fluorescent imaging of phosphatidylserine-rich surfaces using fluorescently labeled annexin V in fixed thrombi (Figure 1B, right; Figure I in the [online-only Data Supplement](#)). These observations were not limited to the FeCl_3 -induced artery injuries. Indeed, the procoagulant platelets were also found preferentially at the surface of thrombi induced via a mechanical injury of abdominal aorta (Figure II in the [online-only Data Supplement](#)), suggesting that the peripheral localization of procoagulant platelets is robust and reproducible between the large-artery thrombosis models.

Procoagulant Platelets Are Also Found at the Surface of Thrombi Formed Ex Vivo

To determine the mechanisms responsible for the peripheral distribution of procoagulant platelets, we next turned to the model of ex vivo thrombus formation.¹⁷ Citrated human blood was supplemented with fluorescent probes, recalcified, and perfused over a collagen layer. After 7 minutes, epifluorescent images of phosphatidylserine-rich surfaces and fibrin were obtained using fluorescently labeled annexin V and antifibrin antibodies, respectively. In line with recent reports, procoagulant platelets formed a ring-like pattern around the contracted thrombi (Figure 2A, left). Interestingly, fibrin was also localized predominantly at the thrombi surfaces, forming prominent ring-like structures (Figure 2A, center). The surface distribution of procoagulant platelets was observed in our ex vivo system for a wide range of experimental conditions (Figure IIIA–IIID in the [online-only Data Supplement](#)): using blood drawn from different organisms (human and murine blood), with different shear rates (200 s^{-1} and 1000 s^{-1}), blood anticoagulants (citrate or hirudin), or experimental temperature

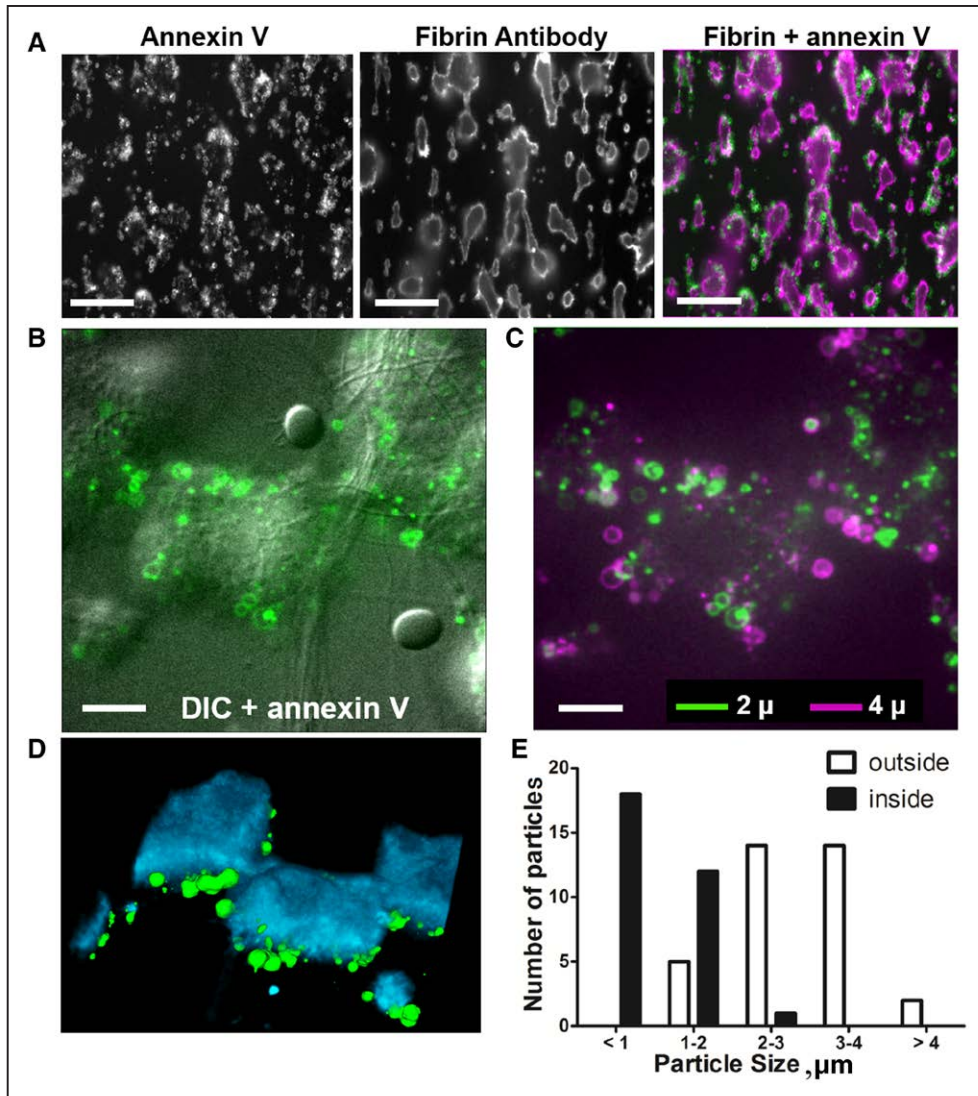


Figure 2. Spatial distribution of procoagulant platelets in a thrombus formed ex vivo. **A**, Citrated recalcified human blood was perfused over collagen for 7 min at 1000 s^{-1} and imaged with epifluorescence microscopy. Fluorescently labeled fibrin antibody and annexin V were added to whole blood just before the perfusion. The **left** image corresponds to annexin V signal, the **middle** image corresponds to fibrin antibody fluorescence channel, whereas the **right** image corresponds to superposition of both images with annexin V signal shown green and fibrin signal shown purple. The scale bar is $50\ \mu\text{m}$ in length. **B**, Thrombi were formed during perfusion of citrated recalcified human blood in a parallel-plate flow chamber over collagen at 200 s^{-1} for 7 min and imaged with confocal microscope. Fluorescently labeled annexin V was added to the whole blood just before perfusion. Superposition of the differential interference contrast (DIC) image of typical thrombus formed on collagen with annexin V–Alexa 647 fluorescence channel. Both images represent optical slices taken at $2\ \mu\text{m}$ height above the collagen-bearing surface. The scale bar is $10\ \mu\text{m}$ in length. **C**, Superposition of 2 images in annexin V–Alexa 647 channel taken at 2 (green) and 4 (purple) μm above the collagen surface. The scale bar is $10\ \mu\text{m}$ in length. **D**, Optical reconstruction of thrombus structure with annexin V–Alexa 647 fluorescence signal (green) and signal from fluorescein isothiocyanate–labeled fibrin(ogen) antibody (blue; Movies I and II in the [online-only Data Supplement](#)). **E**, Distribution of sizes measured for fluorescent objects detected outside (white) and inside (black) the dense part of the thrombus near the collagen surface. Thrombus contours were built using the DIC channel. Analysis was performed using data from $n=5$ experiments. The total numbers N of corresponding fluorescent objects are shown. The distributions are significantly different ($P<0.01$).

(room temperature and physiological 37°C), indicating that such distribution is a robust feature of formed thrombi.

To investigate the distribution of procoagulant surfaces in more detail, we used high-resolution confocal microscopy to image fluorescently labeled annexin V, a marker for high level of phosphatidylserine externalization. Multiple 2-dimensional optical slices were obtained, and the 3-dimensional reconstructions were created using optical tomography. Typical thrombus architecture visualized 7 minutes after starting the perfusion of recalcified citrated blood is shown in Figure 2B and 2C. The procoagulant

platelets are visible as annexin V–positive balloon-shaped particles, most of which localize to the thrombi periphery: around contracted thrombus body (Figure 2C and 2D, Movie I in the [online-only Data Supplement](#)). In particular, these large balloons are often observed at the boundary between the thrombus and collagen layer (Figure IV in the [online-only Data Supplement](#)). Numerous small annexin-positive particles can also be seen, but interestingly, they are found throughout the thrombi (Figure 2B and 2E; Movie II in the [online-only Data Supplement](#)). Thus, prominent absence of procoagulant platelets inside the contracted thrombus could

not be explained by a problem with annexin V penetration and labeling, and the results from ex vivo system mirror the findings from physiological models (Figure 1; Figure I in the [online-only Data Supplement](#)).

Outward Translocation of Procoagulant Platelets Is Responsible for Their Surface Localization

To clarify the origin of the peripheral distribution of procoagulant platelets, we next investigated their localization during thrombus formation in real time. Although some of the annexin V-positive platelets were found at the surface of a growing thrombus, a subset of platelets acquired annexin V marker

inside the thrombus. Interestingly, the real-time imaging revealed that those procoagulant platelets inside the thrombus were not stationary but translocated towards the surface of contracting thrombi (Figure 3A, Movie III in the [online-only Data Supplement](#)). Some of these cells were observed to move against the blood flow, so their translocation could not have been caused by a hydrodynamic drag (Figure 3A and 3B). The outward motion of the procoagulant platelets is especially remarkable because the proaggregatory platelets, labeled with fluorescent anti-CD42b antibody, were observed moving in opposite direction because of thrombus contraction. Indeed, Figure 3B and Movie IV in the [online-only Data](#)

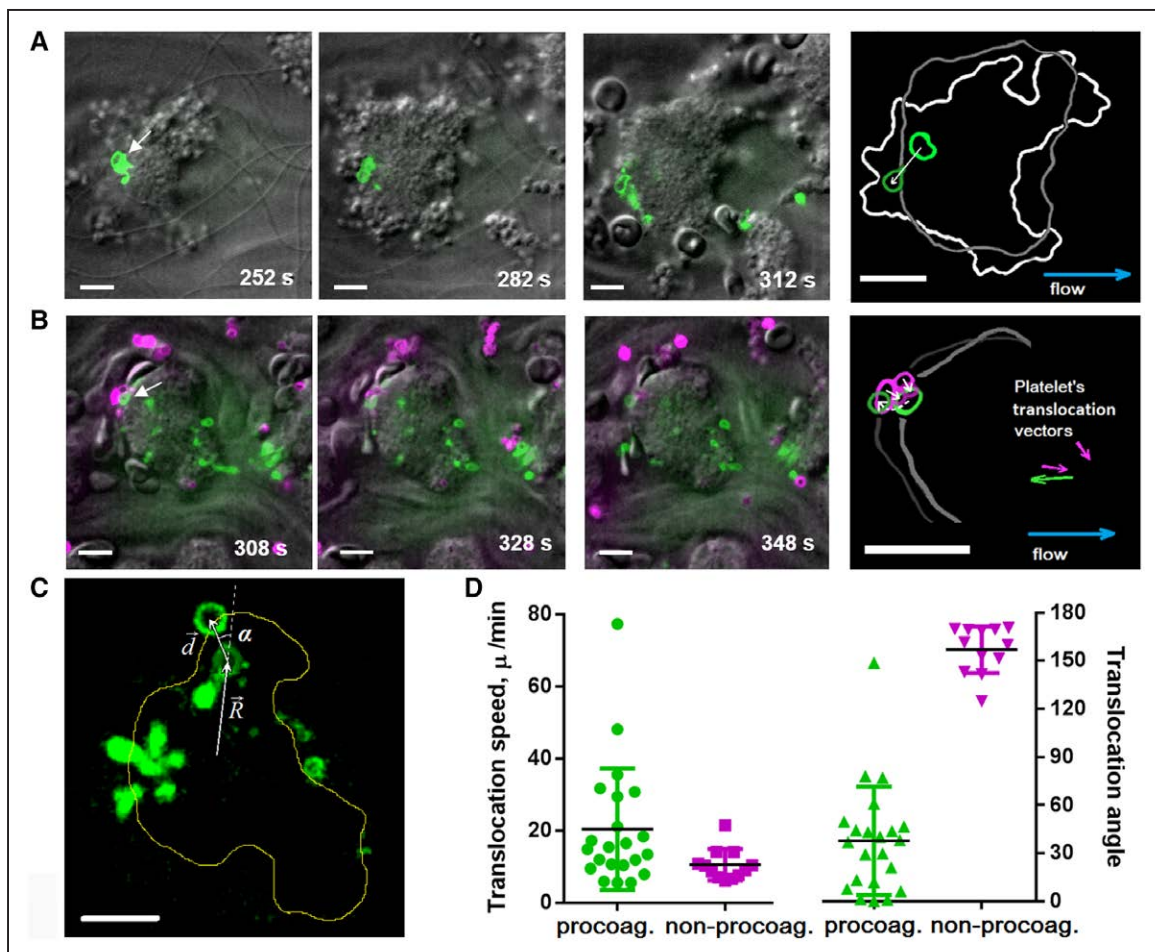


Figure 3. Dynamics of single procoagulant platelets translocation during thrombus formation. Experimental conditions were identical to those described in Figure 1B. **A**, Three images (from left to right) represent temporal sequence of merged confocal images taken 30 s apart (full sequence of images is given in Movie III in the [online-only Data Supplement](#)). Differential interference contrast (DIC) channel is shown in grayscale, whereas annexin V–Alexa 647 fluorescence is shown in green. The fourth image shows schematic and zoomed superposition of the first and last images, in which thrombus contours are presented in grayscale, and procoagulant platelet contours are shown in green. The brightest contours correspond to the first image, whereas dimmer curves correspond to the third image. The scale bars are 10 μ in length. **B**, Three images from left to right are confocal images taken 20 s apart (Movie IV in the [online-only Data Supplement](#)). DIC channel is shown in grayscale, annexin V fluorescence in green, and CD42b antibody in purple. As far as fluorescein isothiocyanate (FITC) dye conjugated with CD42b antibody possesses fast photobleaching kinetics, only newcomer platelets were detected. The last image shows schematic superposition of the first and third images, where thrombus contours are depicted using grayscale, whereas annexin V and CD42b channels are shown in green and purple colors, respectively. Brighter colors correspond to the first image. The scale bars are 10 μ in length. **C**, Image illustrating the principle of quantitative platelet translocation analysis and showing superposition of initial image in annexin V channel (procoagulant platelet is inside the dense part of the thrombus shown with yellow contour) and final image. Translocation vector d shows the total displacement of platelet, whereas average translocation velocity magnitude is determined as the module of displacement vector d divided by corresponding time interval. The translocation angle α is determined as the absolute value of angle between initial platelet position vector R (relative to thrombus center) and translocation vector d . Thus, small angles ($\alpha < 90^\circ$) correspond to outward motion, whereas angles $> 90^\circ$ correspond to inward motion. **D**, Results of quantitative analysis of procoagulant (green) and nonprocoagulant (purple) platelet translocation velocities and angles. Only translocating procoagulant objects with initial position inside dense thrombus were tracked. Total of $n=11$ experiments was analyzed. Translocation of nonprocoagulant platelets was analyzed using anti-CD42b-FITC antibody channel. The difference in translocation speeds and angles between 2 types of platelets was statistically significant ($P < 0.01$).

Supplement illustrate the inward motion of a proaggregatory platelet within the same thrombus that contains a procoagulant platelet moving towards its periphery. Further analysis of the spatial dynamics of these 2 subpopulations revealed that although these cells move in opposite directions, their velocities are similar (Figure 3C and 3D), suggesting a similar mechanism of translocation.

We observed that annexin V–positive microparticles detected inside the thrombus (Figure 1B; Movie II in the online-only Data Supplement) were shed from procoagulant platelets at the early stages of their formation and translocation (Figure VA and VB and Movies III, V, and VI in the online-only Data Supplement). To test whether some procoagulant platelets may form and translocate through the

thrombus earlier than they are observed using fluorescent annexin V marker, we performed experiments with both annexin V and intracellular calcium sensor Fura Red. These experiments revealed that a subset of platelets possessing high calcium levels translocated towards the thrombus surface before annexin V binding was detected on their surface (Figure VC and Movie VII in the online-only Data Supplement). This result explains why some of procoagulant platelets appeared already at the thrombus surface when imaged with fluorescent annexin V marker.

Thus, our results indicate that the specific surface distribution of procoagulant platelets results from a dynamic process involving their outward translocation during thrombus formation.

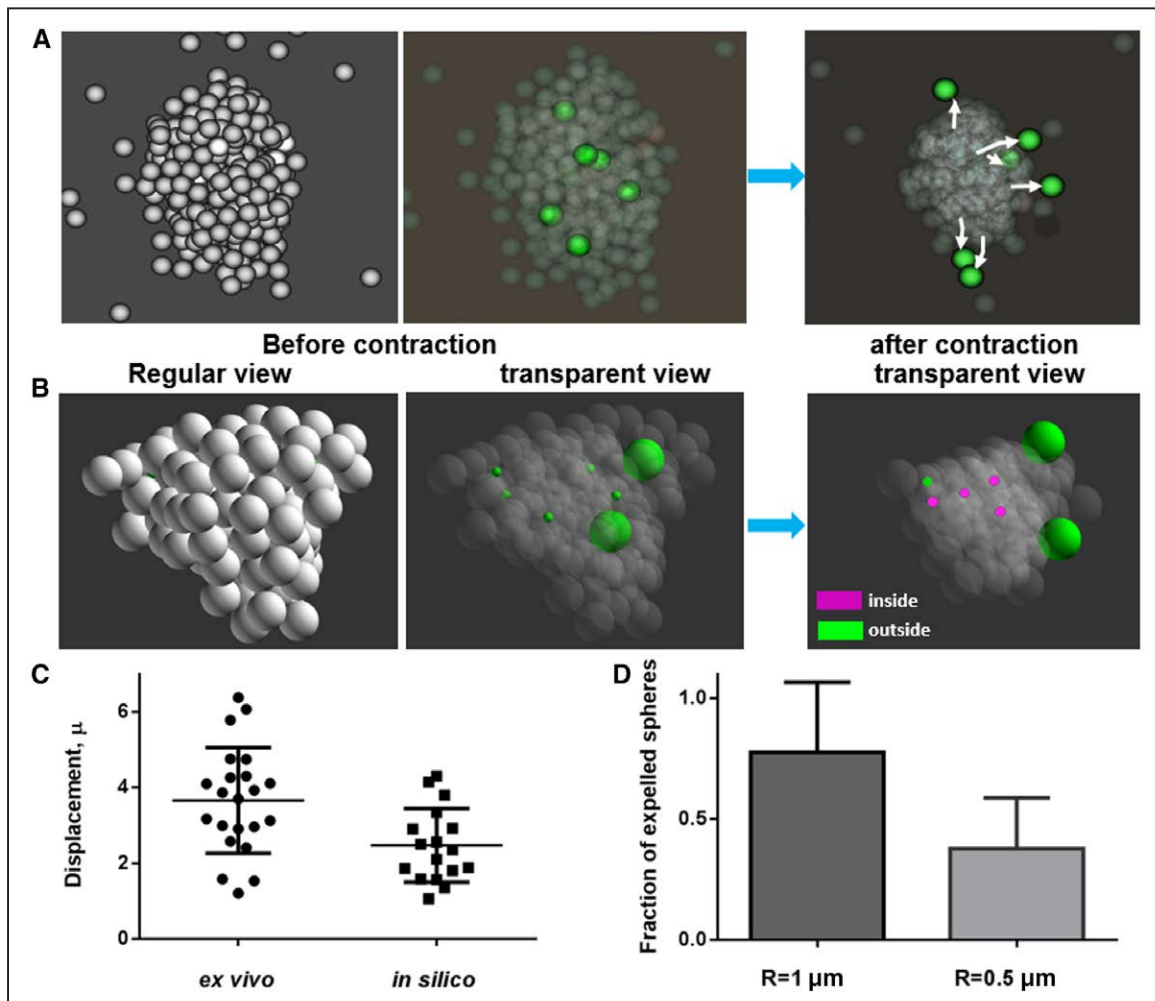


Figure 4. Computational modeling of contraction-driven extrusion of procoagulant platelets. **A**, First image shows the architecture of thrombus consisting of interacting spheres shown in gray before contraction. The second image corresponds to transparent view of thrombus: spheres which do not participate in contraction process (thus mimicking procoagulant platelets) are shown in green color. The third image corresponds to the snapshot taken after contraction process. Arrows depict approximate paths of procoagulant spheres movement to thrombus exterior. **B**, Results of computational modeling of thrombus contraction with spheres of different diameters: 5 spheres of 0.5 micron diameter and 2 spheres of 2 μ diameter were initially chosen inside the thrombus which did not participate in contraction process, thus, mimicking procoagulant objects of various sizes. First image shows the architecture of thrombus consisting of interacting spheres shown in gray and procoagulant spheres shown in green. The second image corresponds to transparent view of thrombus. The third image corresponds to the snapshot taken after contraction process. Smaller spheres, which stayed inside thrombus, are shown in purple color, whereas spheres outside the contracted thrombus are shown in green. **C**, Outward displacements of procoagulant objects measured ex vivo and corresponding data from in silico experiments (combined for $R=1 \mu$ and $R=0.5 \mu$ particles). **D**, Statistical analysis of the percentage of expelled spheres with diameter of 2 and 1 μ . For each numerical experiment, random spheres were chosen that would not participate in contraction process. The rest of the spheres were involved in contraction and had 2 μ diameters in all simulations. The percentage of expelled spheres was determined as the ratio of the number of expelled spheres to the total number of spheres initially located inside the aggregate. $n=7$ simulations were performed for each size of the noncontracting spheres, and the difference of the ratios was statistically significant for 2 groups of data corresponding to different sizes of noncontracting spheres (Mann-Whitney U test, $P<0.05$).

Thrombus Contraction Drives Outward Translocation of Procoagulant Platelets

Procoagulant platelets could translocate through thrombus either by active motility or passively; however, both calpain-dependent degradation of cytoskeleton¹⁶ and integrin inactivation⁵ reported for this subpopulation make their translocation through autonomous motility rather unlikely. A passive motility mechanism seems feasible because mechanical forces acting within multicellular aggregates have previously been shown to drive cell extrusion in other tissues.³⁶ Consistently, in our experiments, we observed that during thrombus contraction, some red blood cells trapped inside thrombus become extruded, appearing to translocate toward periphery (Movie VIII in the [online-only Data Supplement](#)).

To examine whether a similar mechanism could lead to the displacement of the procoagulant platelets, we first used theoretical approaches. We modeled a contracting thrombus as a system of 2- μm spheres interacting with Morse potential thus mimicking the interacting proaggregatory platelets (Figure 4A). Additional spheres that experienced the elastic repulsion and weak interaction with proaggregate spheres were introduced into this mechanical system to mimic the procoagulant platelets that weakly adhere to each other or to other platelets.⁴ After simulation starts, the adhering spheres move closer together (Figure 4A), mirroring the increase in platelet packing density during the contraction observed both ex vivo and in vivo.^{8,37} However, the procoagulant-platelets-representing-spheres become extruded and translocate to the outer surface (Figure 4A and 4B; Movie IX in the [online-only Data Supplement](#)). The mean outward displacement of these spheres was similar to the experimentally observed displacements of the annexin V-labeled objects in our ex vivo system (Figure 4C). Efficient extrusion of procoagulant spheres was observed only when their interactions with proaggregatory spheres was much weaker than interaction between proaggregatory spheres (Figure X in the [online-only Data Supplement](#)). Computational analysis also revealed that the efficiency of mechanical extrusion was significantly lower for the particles with smaller diameter: only 38% of 1- μm spheres were expelled to thrombus surface, whereas this fraction for the 2- μm spheres was 78% (Figure 4D). Smaller spheres (0.5 μm in diameter), which mimicked the annexin V-positive microparticles, were extruded even less efficiently (Figure 4B), consistent with our ex vivo experiments (Figure 2E). Thus, these in silico results demonstrate that thrombus contraction can drive specific extrusion of the procoagulant platelets while leaving their small microparticles inside the thrombus.

Based on the above results, we predicted that surface localization of the procoagulant platelets should be significantly reduced if thrombus contraction is defective. To test this prediction, we used blood from the *MYH9*-deficient mice lacking nonmuscle myosin heavy chain IIa that is specifically expressed in megakaryocytes and platelets.³⁸ Previous studies have established that thrombus contraction and hemostasis were severely compromised in these mice, whereas aggregation and secretion were normal.³⁸ Formation of procoagulant platelets in response to potent activation in these mice was similar to that observed in wild-type (WT) mice under most conditions (Figure VI in the [online-only Data Supplement](#)).

Annexin V-labeling was used to compare the distributions of procoagulant platelets in the thrombi formed ex vivo in the blood derived from mutant versus WT mice. The surface of the WT thrombi exhibited high annexin V staining because of the presence of procoagulant platelets. Total annexin V intensity of the inner thrombus core was also high because of the fluorescence of microparticles (Figure 5A and 5B). In contrast, thrombi formed in blood of the *MYH9*-deficient mice contained randomly distributed annexin V-positive cells, leading to a low ratio of the fluorescence intensity at the surface and inside the thrombi (Figure 5B). Thus, these experiments strongly suggest that thrombus contraction drives the outward displacement of procoagulant platelets.

Translocation of Procoagulant Platelets Controls Spatial Distribution of Fibrin

Next, we investigated functional significance of the peripheral localization of procoagulant platelets. As described earlier in this article, fibrin becomes enriched at the surface of thrombi formed in human blood ex vivo (Figure 2A), giving an appearance of colocalization with procoagulant platelets. Importantly, the arrival of procoagulant platelets preceded the increase in fibrin signal, suggesting that fibrin formation was boosted after these procoagulant cells were extruded to the thrombi surface (Movie X in the [online-only Data Supplement](#)). Similar experiments with WT murine blood demonstrated that just as in human blood, both fibrin and procoagulant platelets were clearly seen as rings around the WT murine thrombi (Figure 5C). The observed surface distribution of fibrin is unlikely to result from steric hindrance to antibody penetration because we obtained strong labeling of the activated platelets inside the thrombi using anti-P-selectin antibodies of the same type (Figure VII in the [online-only Data Supplement](#)). However, the colocalization of procoagulant platelets and fibrin in murine blood was not complete: fibrin was sometimes enriched at the sites with no annexin V signal, whereas some annexin V-positive locations were fibrin-free (Figures 5C and 2A). This mislocalization could arise from diffusion and convection-mediated transport of thrombin from the sites of its production. Indeed, similar effect was obtained in a mathematical model that incorporates thrombin flux at some fixed sites, biochemical reaction of thrombin-dependent fibrin generation,^{38a,b} and convection and diffusion of thrombin and fibrin monomers (Figure VIII in the [online-only Data Supplement](#)).

To verify whether peripheral distribution of procoagulant platelets and fibrin is independent on the presence of the tissue factor, we perfused human recalcified blood over surface covered with both tissue factor^{38c} and type I collagen. In line with results obtained in the absence of tissue factor, procoagulant platelets formed specific surface distribution (Figure IX and Movie XI in the [online-only Data Supplement](#)). Importantly, fibrin generation in this case also originated from the thrombus surface (Figure IX and Movie XI in the [online-only Data Supplement](#)).

To further test whether the extrusion of procoagulant platelets could cause fibrin enrichment at thrombus periphery, we investigated whether such localization can be abolished by disrupting extrusion of procoagulant platelets. To address this question, we used blood from the *MYH9*-knockout mice,

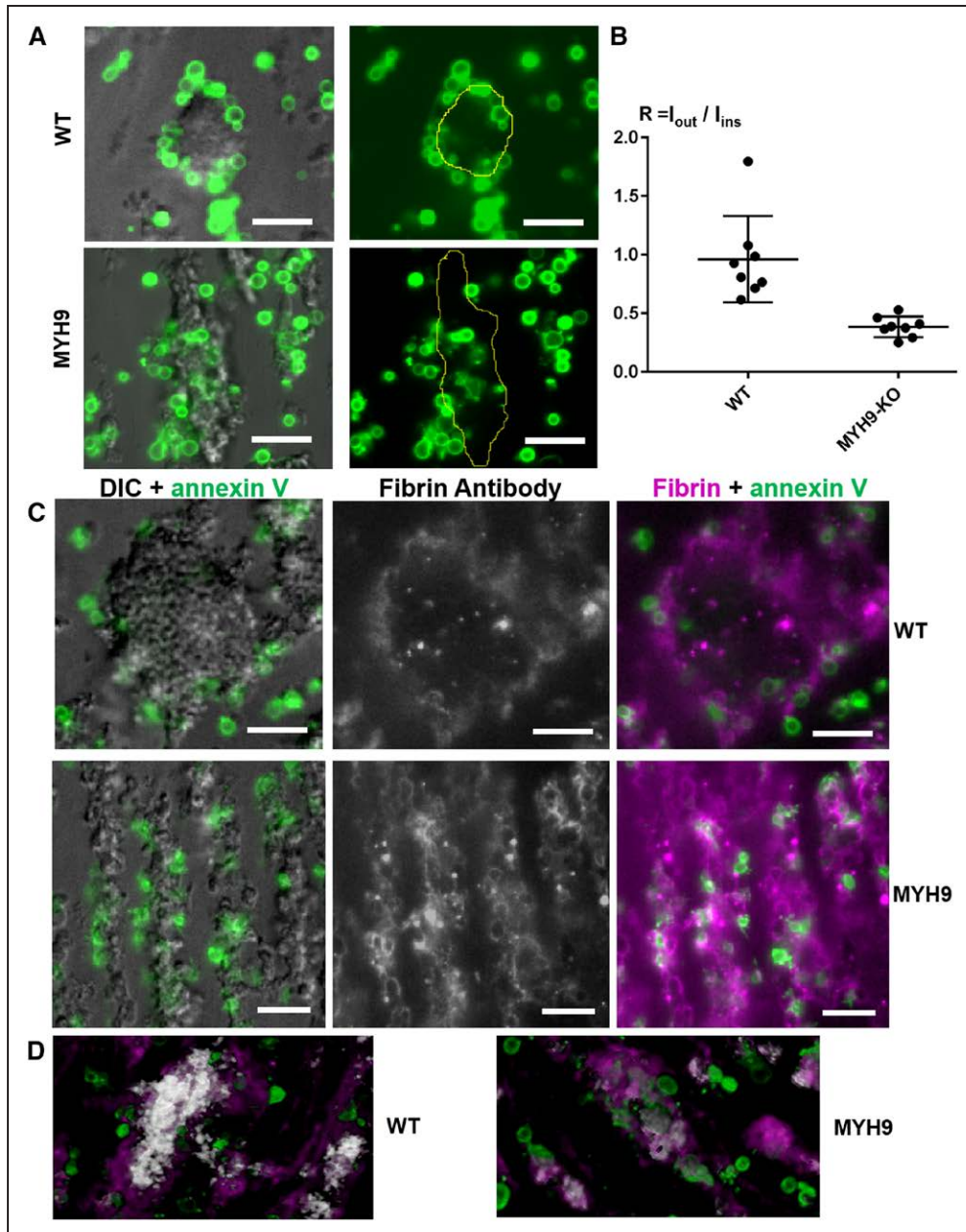


Figure 5. Spatial distribution of procoagulant platelets and fibrin obtained with blood of wild-type (WT) and *MYH9*-knockout (KO) mice. **A, Higher:** hirudinized WT murine blood was perfused over collagen at 1000 s^{-1} for 5 min. Fluorescently labeled annexin V was added to blood just before the perfusion. First image from the **left** shows superposition of differential interference contrast (DIC) channel shown in grayscale, and annexin V fluorescence shown in green. **Right** image shows annexin V channel with yellow curve corresponding to thrombus contour which was built manually using only the DIC channel. **Lower:** similar results obtained with blood of *MYH9*-deficient mice. All scale bars are $10 \mu\text{m}$. **B,** Analysis of annexin V–Alexa 647 fluorescence distribution in thrombi formed using blood WT and *MYH9*-KO mice. R value was calculated as the ratio of total fluorescence measured in annexin V channel for the region outside the dense thrombus (including procoagulant platelets outside the dense core) to the same value measured for the inside part of the thrombus (region inside the yellow contours shown in **A**). The plot represents summarized data for $n=8$ thrombi of WT mice and $n=8$ thrombi for *MYH9*-KO mice. Mann-Whitney U test showed significant difference between R values ($P<0.01$). **C,** Recalcified citrated WT murine blood was perfused over collagen at 1000 s^{-1} for 5 min. Fluorescently labeled annexin V and antifibrin antibody were added to blood just before the perfusion. Labels above show the corresponding channels (DIC and epifluorescence regime). Three similar images below demonstrate the results obtained with blood of *MYH9*-deficient mice. **D,** Citrated recalcified murine blood was perfused over collagen for 7 min at 1000 s^{-1} . Platelets were labeled with DiOC6 (3,3'-dihexyloxycarbocyanine iodide), whereas fluorescently labeled fibrin antibody and annexin V were added to whole blood just before the perfusion. The **left** image corresponds to 3-dimensional optical reconstruction of WT thrombi showing fibrin signal in purple, platelet signal in white, and annexin V signal in green. Image to the **right** corresponds to optical reconstruction of thrombus obtained with blood of *MYH9*-KO mouse (Movie XII in the [online-only Data Supplement](#)).

in which the procoagulant platelets form normally but fail to translocate to the thrombi surface. Under these conditions, diffuse fibrin signal was detected both around and inside the uncontracted thrombi (Figure 5C). Using 3-dimensional

optical reconstructions, we found a strikingly different composition of thrombi in the *MYH9*-knockout versus WT blood. Instead of encircling the dense thrombus core, the procoagulant platelets and fibrin in mutant blood formed a homogeneous

mixture with regular activated platelets (Figure 5D; Movie XII in the [online-only Data Supplement](#)). Thus, the mechanical extrusion of procoagulant platelets from the contracting thrombus leads to the surface distribution of fibrin.

Discussion

Here, we show that procoagulant platelets are located peripherally in thrombi formed using FeCl_3 -induced thrombosis of carotid artery or mechanical injury of the aorta. Our ex vivo experiments reveal a mechanism wherein procoagulant platelets are mechanically expelled to the outer surface of the thrombus by the contraction process. Such extrusion of procoagulant platelets results in their ring-like distribution around thrombus and leads to surface-enhanced generation of fibrin ex vivo.

Surface distribution of procoagulant platelets was observed here within a wide range of experimental conditions ex vivo and in 2 in vivo models and is consistent with the ex vivo data of Munnix et al¹⁹ and in vivo data of Yuan et al,³⁰ as well as earlier reports describing the morphology of hemostatic plugs.^{31,32} Contraction-driven displacement of procoagulant platelets to thrombus surface explains the disagreement between the requirement of high activation for procoagulant platelets, which should be expected at thrombus core and their observation outside the main contracted thrombus body. Importantly, the generally accepted core-and-shell model of thrombus heterogeneity⁸ suggests the contraction process to be the driving force of thrombus core formation.³⁹ Thus, the phenomenon of procoagulant platelets extrusion can occur within the core region of thrombus.

The mechanism of procoagulant platelet expulsion agrees with reports on the decreased adhesivity of procoagulant platelets^{4,12} and their disrupted cytoskeleton¹⁶ that are both likely to contribute to this phenomenon. Mechanical extrusion of both dead and live cells through actomyosin ring contraction in surrounding cells has been established in epithelia and was shown to be crucial for cellular homeostasis.³⁶ Clot contraction-driven extrusion of necrotic procoagulant platelets to thrombus surface can, therefore, represent a more general mechanism of cellular spatial segregation which might have important role beyond hemostasis or thrombosis.

Both translocation speeds and angles measured for procoagulant platelets moving within the thrombus have rather wide range (Figure 3D), likely because of complex mechanical environment within the contracting clot. After leaving the internal part of the thrombus, most procoagulant platelets stayed within the surface (Movies III–V in the [online-only Data Supplement](#)) thus reflecting the presence of some residual mechanical interactions with proaggregatory platelets. Our in silico simulations suggest that to achieve efficient platelet extrusion by reasonable degree of contraction, the interactions between procoagulant and proaggregatory platelets should be dampened by ≥ 2 orders of magnitude, compared with interactions between the contracting platelets (Figure X in the [online-only Data Supplement](#)). Given the value of forces reached by single contracting platelet⁴⁰ (order of 10 nN), these reduced forces between procoagulant and proaggregatory platelets should be < 100 pN. Interestingly, this upper bound corresponds to rather strong interaction capable of sustaining surface shear rates of

1000 s^{-1} and probably explaining the retention of procoagulant platelet on the surface of forming thrombi.

The consequence of surface distribution of procoagulant platelets reported here is associated with spatial features of coagulation process: fibrin formation occurs on the surface of thrombi formed ex vivo with blood of humans and WT mice, but not in *MYH9*-deficient mice. Thus, surface distribution of procoagulant platelets might be important for platelet-dependent fibrin generation at the base of the thrombus, which is crucial for overall thrombus stability in the flow. Our data on fibrin distribution agree with the recent report of Swieringa et al.⁴¹ Surface distribution of fibrin in thrombi formed in vivo was also reported by Kamocka et al,⁴² but those observations were difficult to correlate with other reports.^{8,29} It is essential that all experimental models in this article use relatively large vessels and timescales (over 5 minutes), consistent with the timescales of in vitro procoagulant platelets formation (5–15 minutes).¹³ This could explain different fibrin distribution⁸ and general lack of procoagulant platelets²⁶ in the experiments using cremaster arteriole. Interestingly, all existing data on fibrin formation in the hemostatic plugs in vivo also report fibrin on the periphery of platelet thrombi,^{32,43,44} despite great differences in the methods and models used. Thus, the mechanism of contraction-driven redistribution of procoagulant platelets described here could be responsible for this specific architectural feature of hemostatic plugs. Although the detailed characterization of this is beyond the scope of the present study, it is tempting to speculate that the fibrin film on the surfaces of hemostatic platelet aggregate, that is formed because of this contraction-driven externalization of procoagulant platelets, could be important for its integrity. In line with this speculation *MYH9* mice, lacking contraction-mediated extrusion of procoagulant platelets, also have impaired hemostasis, despite their other platelet functions being normal.³⁸ A recent study has suggested that fibrin films could be also critical in preventing infection.⁴⁵ Contraction-driven redistribution of procoagulant platelets to thrombus surface might also drive pathophysiological processes, such as formation of neutrophil aggregates, which was recently shown to rely on the interactions between neutrophils and procoagulant platelets.³⁰

Thus, the results of this study demonstrate the importance of contraction process for the displacement of procoagulant platelets to thrombus surface that can be crucial for the spatial control of thrombin generation and fibrin formation.

Sources of Funding

The work was supported by the grant from the endowment fund Doctors, Innovations, Science for Children to M.A. Pantelev, by the Russian Foundation for Basic Research grants 16-04-01163 to D.Y. Nechipurenko, 17-04-01309 and 18-34-20026 to M.A. Pantelev, and by the Russian Federation President Grant to Young Scientists MD-229.2017.4 to M.A. Pantelev and MK-2706.2017.4 to D.Y. Nechipurenko. Computational modeling of thrombus dynamics was performed using the equipment of the shared research facilities of high-performance computing resources at Lomonosov Moscow State University.

Disclosures

None.

References

- Jackson SP. The growing complexity of platelet aggregation. *Blood*. 2007;109:5087–5095. doi: 10.1182/blood-2006-12-027698
- Dale GL. Coated-platelets: an emerging component of the procoagulant response. *J Thromb Haemost*. 2005;3:2185–2192. doi: 10.1111/j.1538-7836.2005.01274.x
- Heemskerk JW, Mattheij NJ, Cosemans JM. Platelet-based coagulation: different populations, different functions. *J Thromb Haemost*. 2013;11:2–16. doi: 10.1111/jth.12045
- Yakimenko AO, Verholomova FY, Kotova YN, Ataulkhanov FI, Pantelev MA. Identification of different proaggregatory abilities of activated platelet subpopulations. *Biophys J*. 2012;102:2261–2269. doi: 10.1016/j.bpj.2012.04.004
- Jackson SP, Schoenwaelder SM. Procoagulant platelets: are they necrotic? *Blood*. 2010;116:2011–2018. doi: 10.1182/blood-2010-01-261669
- Kempton CL, Hoffman M, Roberts HR, Monroe DM. Platelet heterogeneity: variation in coagulation complexes on platelet subpopulations. *Arterioscler Thromb Vasc Biol*. 2005;25:861–866. doi: 10.1161/01.ATV.0000155987.26583.9b
- Munnix IC, Cosemans JM, Auger JM, Heemskerk JW. Platelet response heterogeneity in thrombus formation. *Thromb Haemost*. 2009;102:1149–1156. doi: 10.1160/TH09-05-0289
- Stalker TJ, Traxler EA, Wu J, Wannemacher KM, Cermignano SL, Voronov R, Diamond SL, Brass LF. Hierarchical organization in the hemostatic response and its relationship to the platelet-signaling network. *Blood*. 2013;121:1875–1885. doi: 10.1182/blood-2012-09-457739
- Alberio L, Safa O, Clemetson KJ, Esmon CT, Dale GL. Surface expression and functional characterization of alpha-granule factor V in human platelets: effects of ionophore A23187, thrombin, collagen, and convulxin. *Blood*. 2000;95:1694–1702.
- London FS, Marcinkiewicz M, Walsh PN. PAR-1-stimulated factor IXa binding to a small platelet subpopulation requires a pronounced and sustained increase of cytoplasmic calcium. *Biochemistry*. 2006;45:7289–7298. doi: 10.1021/bi060294m
- Pantelev MA, Ananyeva NM, Greco NJ, Ataulkhanov FI, Saenko EL. Two subpopulations of thrombin-activated platelets differ in their binding of the components of the intrinsic factor X-activating complex. *J Thromb Haemost*. 2005;3:2545–2553. doi: 10.1111/j.1538-7836.2005.01616.x
- Abaeva AA, Canault M, Kotova YN, Obydennyi SI, Yakimenko AO, Podoplelova NA, Kolyadko VN, Chambost H, Mazurov AV, Ataulkhanov FI, Nurden AT, Alessi MC, Pantelev MA. Procoagulant platelets form an α -granule protein-covered “cap” on their surface that promotes their attachment to aggregates. *J Biol Chem*. 2013;288:29621–29632. doi: 10.1074/jbc.M113.474163
- Mattheij NJ, Gilio K, van Kruchten R, Jobe SM, Wieschhaus AJ, Chishti AH, Collins P, Heemskerk JW, Cosemans JM. Dual mechanism of integrin α IIb β 3 closure in procoagulant platelets. *J Biol Chem*. 2013;288:13325–13336. doi: 10.1074/jbc.M112.428359
- Topalov NN, Kotova YN, Vasil'ev SA, Pantelev MA. Identification of signal transduction pathways involved in the formation of platelet subpopulations upon activation. *Br J Haematol*. 2012;157:105–115. doi: 10.1111/j.1365-2141.2011.09021.x
- Mattheij NJ, Swieringa F, Mastenbroek TG, Berny-Lang MA, May F, Baaten CC, van der Meijden PE, Henskens YM, Beckers EA, Suylen DP, Nolte MW, Hackeng TM, McCarty OJ, Heemskerk JW, Cosemans JM. Coated platelets function in platelet-dependent fibrin formation via integrin α IIb β 3 and transglutaminase factor XIII. *Haematologica*. 2016;101:427–436. doi: 10.3324/haematol.2015.131441
- Rukoyatkina N, Begonja AJ, Geiger J, Eigenthaler M, Walter U, Gambaryan S. Phosphatidylserine surface expression and integrin alpha IIb beta 3 activity on thrombin/convulxin stimulated platelets/particles of different sizes. *Br J Haematol*. 2009;144:591–602. doi: 10.1111/j.1365-2141.2008.07506.x
- Artemenko EO, Yakimenko AO, Pichugin AV, Ataulkhanov FI, Pantelev MA. Calpain-controlled detachment of major glycoproteins from the cytoskeleton regulates adhesive properties of activated phosphatidylserine-positive platelets. *Biochem J*. 2016;473:435–448. doi: 10.1042/BJ20150779
- Podoplelova NA, Sveshnikova AN, Kurasawa JH, Sarafanov AG, Chambost H, Vasil'ev SA, Demina IA, Ataulkhanov FI, Alessi MC, Pantelev MA. Hysteresis-like binding of coagulation factors XI/Xa to procoagulant activated platelets and phospholipids results from multistep association and membrane-dependent multimerization. *Biochim Biophys Acta*. 2016;1858:1216–1227. doi: 10.1016/j.bbame.2016.02.008
- Podoplelova NA, Sveshnikova AN, Kotova YN, Eckly A, Receveur N, Nechipurenko DY, Obydennyi SI, Kireev II, Gachet C, Ataulkhanov FI, Mangin PH, Pantelev MA. Coagulation factors bound to procoagulant platelets concentrate in cap structures to promote clotting. *Blood*. 2016;128:1745–1755. doi: 10.1182/blood-2016-02-696898
- Munnix IC, Kuijpers MJ, Auger J, Thomassen CM, Panizzi P, van Zandvoort MA, Rosing J, Bock PE, Watson SP, Heemskerk JW. Segregation of platelet aggregatory and procoagulant microdomains in thrombus formation: regulation by transient integrin activation. *Arterioscler Thromb Vasc Biol*. 2007;27:2484–2490. doi: 10.1161/ATVBAHA.107.151100
- Fujii T, Sakata A, Nishimura S, Eto K, Nagata S. Tmem16f is required for phosphatidylserine exposure and microparticle release in activated mouse platelets. *Proc Natl Acad Sci USA*. 2015;112:12800–12805.
- Daskalakis M, Colucci G, Keller P, Rochat S, Silzle T, Biasiutti FD, Barizzi G, Alberio L. Decreased generation of procoagulant platelets detected by flow cytometric analysis in patients with bleeding diathesis. *Cytometry B Clin Cytom*. 2014;86:397–409. doi: 10.1002/cyto.b.21157
- Prodan CI, Stoner JA, Dale GL. Acute hemorrhagic complications are associated with lower coated-platelet levels in non-lacunar brain infarction. *J Thromb Haemost*. 2015;13:2233–2239. doi: 10.1111/jth.13160
- Saxena K, Pethe K, Dale GL. Coated-platelet levels may explain some variability in clinical phenotypes observed with severe hemophilia. *J Thromb Haemost*. 2010;8:1140–1142. doi: 10.1111/j.1538-7836.2010.03828.x
- Kirkpatrick AC, Stoner JA, Dale GL, Prodan CI. Elevated coated-platelets in symptomatic large-artery stenosis patients are associated with early stroke recurrence. *Platelets*. 2014;25:93–96. doi: 10.3109/09537104.2013.775570
- Kirkpatrick AC, Tafur AJ, Vincent AS, Dale GL, Prodan CI. Coated-platelets improve prediction of stroke and transient ischemic attack in asymptomatic internal carotid artery stenosis. *Stroke*. 2014;45:2995–3001. doi: 10.1161/STROKEAHA.114.006492
- Hua VM, Abeynaike L, Glaros E, Campbell H, Pasalic L, Hogg PJ, Chen VM. Necrotic platelets provide a procoagulant surface during thrombosis. *Blood*. 2015;126:2852–2862. doi: 10.1182/blood-2015-08-663005
- Jobe SM, Wilson KM, Leo L, Raimondi A, Molkentin JD, Lentz SR, Di Paola J. Critical role for the mitochondrial permeability transition pore and cyclophilin D in platelet activation and thrombosis. *Blood*. 2008;111:1257–1265. doi: 10.1182/blood-2007-05-092684
- Kulkarni S, Jackson SP. Platelet factor XIII and calpain negatively regulate integrin α IIb β 3 adhesive function and thrombus growth. *J Biol Chem*. 2004;279:30697–30706. doi: 10.1074/jbc.M403559200
- Hayashi T, Mogami H, Murakami Y, Nakamura T, Kanayama N, Konno H, Urano T. Real-time analysis of platelet aggregation and procoagulant activity during thrombus formation in vivo. *Pflugers Arch*. 2008;456:1239–1251. doi: 10.1007/s00424-008-0466-9
- Yuan Y, Alwis I, Wu MCL, Kaplan Z, Ashworth K, Bark D Jr, Pham A, McFadyen J, Schoenwaelder SM, Josefsson EC, Kile BT, Jackson SP. Neutrophil macroaggregates promote widespread pulmonary thrombosis after gut ischemia. *Sci Transl Med*. 2017;9:eaam5861. doi: 10.1126/scitranslmed.aam5861
- Jørgensen L, Borchgrevink CF. The platelet plug in normal persons. *Acta Pathol Microbiol Scand*. 1963;57:40–56.
- Hovig T, Rowsell HC, Dodds WJ, Jørgensen L, Mustard JF. Experimental hemostasis in normal dogs and dogs with congenital disorders of blood coagulation. *Blood*. 1967;30:636–668.
- Schaff M, Tang C, Maurer E, et al. Integrin α 6 β 1 is the main receptor for vascular laminins and plays a role in platelet adhesion, activation, and arterial thrombosis. *Circulation*. 2013;128:541–552. doi: 10.1161/CIRCULATIONAHA.112.000799
- Eckly A, Hechler B, Freund M, Zerr M, Cazenave JP, Lanza F, Mangin PH, Gachet C. Mechanisms underlying FeCl₃-induced arterial thrombosis. *J Thromb Haemost*. 2011;9:779–789. doi: 10.1111/j.1538-7836.2011.04218.x
- Yazdani A, Li H, Humphrey JD, Kamiadakis GE. A general shear-dependent model for thrombus formation. *PLoS Comput Biol*. 2017;13:e1005291. doi: 10.1371/journal.pcbi.1005291
- Hess MW, Siljander P. Procoagulant platelet balloons: evidence from cryopreparation and electron microscopy. *Histochem Cell Biol*. 2001;115:439–443.
- Eisenhoffer GT, Loftus PD, Yoshigi M, Otsuna H, Chien CB, Morcos PA, Rosenblatt J. Crowding induces live cell extrusion to maintain homeostatic cell numbers in epithelia. *Nature*. 2012;484:546–549. doi: 10.1038/nature10999

37. Ono A, Westein E, Hsiao S, Nesbitt WS, Hamilton JR, Schoenwaelder SM, Jackson SP. Identification of a fibrin-independent platelet contractile mechanism regulating primary hemostasis and thrombus growth. *Blood*. 2008;112:90–99. doi: 10.1182/blood-2007-12-127001
38. Léon C, Eckly A, Hechler B, et al. Megakaryocyte-restricted MYH9 inactivation dramatically affects hemostasis while preserving platelet aggregation and secretion. *Blood*. 2007;110:3183–3191. doi: 10.1182/blood-2007-03-080184
- 38a. Mihalyi E. Clotting of bovine fibrinogen. Kinetic analysis of the release of fibrinopeptides by thrombin and of the calcium uptake upon clotting at high fibrinogen concentrations. *Biochemistry*. 1988;27:976–982.
- 38b. Shibeko AM, Lobanova ES, Pantelev MA, Ataulkhanov FI. Blood flow controls coagulation onset via the positive feedback of factor VII activation by factor Xa. *BMC Syst Biol*. 2010;4:5. doi: 10.1186/1752-0509-4-5
- 38c. Fadeeva OA, Pantelev MA, Karamzin SS, Balandina AN, Smirnov IV, Ataulkhanov FI. Thromboplastin immobilized on polystyrene surface exhibits kinetic characteristics close to those for the native protein and activates in vitro blood coagulation similarly to thromboplastin on fibroblasts. *Biochemistry (Mosc)*. 2010;75:734–743.
39. Stalker TJ, Welsh JD, Tomaiuolo M, Wu J, Colace TV, Diamond SL, Brass LF. A systems approach to hemostasis: 3. Thrombus consolidation regulates intrathrombus solute transport and local thrombin activity. *Blood*. 2014;124:1824–1831. doi: 10.1182/blood-2014-01-550319
40. Lam WA, Chaudhuri O, Crow A, Webster KD, Li TD, Kita A, Huang J, Fletcher DA. Mechanics and contraction dynamics of single platelets and implications for clot stiffening. *Nat Mater*. 2011;10:61–66. doi: 10.1038/nmat2903
41. Swieringa F, Baaten CC, Verdoold R, Mastenbroek TG, Rijnveld N, van der Laan KO, Breel EJ, Collins PW, Lancé MD, Henskens YM, Cosemans JM, Heemskerk JW, van der Meijden PE. Platelet control of fibrin distribution and microelasticity in thrombus formation under flow. *Arterioscler Thromb Vasc Biol*. 2016;36:692–699. doi: 10.1161/ATVBAHA.115.306537
42. Kamocka MM, Mu J, Liu X, Chen N, Zollman A, Sturonas-Brown B, Dunn K, Xu Z, Chen DZ, Alber MS, Rosen ED. Two-photon intravital imaging of thrombus development. *J Biomed Opt*. 2010;15:016020.
43. French JE, Macfarlane RG, Sanders AG. The structure of haemostatic plugs and experimental thrombi in small arteries. *Br J Exp Pathol*. 1964;45:467–474.
44. Getz TM, Piatt R, Petrich BG, Monroe D, Mackman N, Bergmeier W. Novel mouse hemostasis model for real-time determination of bleeding time and hemostatic plug composition. *J Thromb Haemost*. 2015;13:417–425. doi: 10.1111/jth.12802
45. Macrae FL, Duval C, Papareddy P, et al. A fibrin biofilm covers blood clots and protects from microbial invasion. *J Clin Invest*. 2018;128:3356–3368. doi: 10.1172/JCI98734

Highlights

- Procoagulant platelets are predominantly localized at thrombus surface.
- Surface distribution of procoagulant platelets is a result of their contraction-driven extrusion from the inner layers of the thrombus.
- Such distribution of procoagulant platelets results in surface-enhanced generation of fibrin.